Journal of Materials and Environmental Science
ISSN : 2028-2508
e-ISSN : 2737-890X
CODEN : JMESCN

J. Mater. Environ. Sci., 2025, Volume 16, Issue 2, Page 304-319

http://www.jmaterenvironsci.com

Evaluation of Corrosion Inhibition Potential of Schiff Bases Derived from 2-Hydroxybenzaldehyde on Mild Steel in 1M HCl Solution

Magaji Ladan[1*], Zakariyya Danyaro[2] and Ayuba Abdullahi Muhammad[1]

Department of Pure and Industrial Chemistry, Faculty of Physical Sciences, Bayero University, Kano, P. M. B. 3011, Nigeria

[2]Department of Chemistry, Jigawa State College of Remedial and Advanced Studies Babura, Jigawa State.

**Corresponding author, Email address: mladan.chm@buk.edu.ng*

Received *21 Jan 2025,*
Revised *11 Feb 2025,*
Accepted *12 Feb 2025*

Keywords:
- ✓ *Schiff base;*
- ✓ *Weight loss;*
- ✓ *Potentiodynamic polarization;*
- ✓ *Corrosion inhibition;*
- ✓ *Mild steel*

Citation*: Ladan M., Ayuba A. M., Zakariyya D. (2025) Evaluation of Corrosion Inhibition Potential of Schiff Bases Derived from 2-Hydroxybenzaldehyde on Mild Steel in 1M HCl Solution, J. Mater. Environ. Sci., 16(2), 304-319*

Abstract: This study explored the corrosion inhibition effect of 2-[2-(hydroxybenzylide)amino]benzanoic acid (SB1) and (2-hydroxybenzylidene)-(2-hydroxyphenyl) amine (SB2) Schiff bases on mild steel in 1M HCl solution using weight loss and potentiodynamic polarization (PDP) techniques under varying conditions of immersion time, inhibitor concentration, and temperature. Fourier Transform Infrared Spectroscopy (FTIR) and Scanning Electron Microscopy (SEM) techniques characterised the Schiff bases and the resulting corrosion products. The results indicated that inhibition efficiency increased with higher concentrations of the Schiff bases but decreased with rising temperatures and SB1 with inhibition efficiency of 89.98 % is relatively higher than that of SB2 with 88.03 %. PDP analysis revealed that the Schiff bases primarily suppressed anodic reactions, functioning as an anodic-type inhibitor. The Langmuir isotherm best described the adsorption behavior of the Schiff bases on the mild steel surface. Thermodynamic and kinetic parameters confirmed a strong interaction between the Schiff base and the mild steel surface. FTIR and SEM analyses further confirmed the nature of interaction of inhibitor molecules on the steel surface. These findings established that the Schiff bases are effective corrosion inhibitors for mild steel in a 1M HCl solution.

1. Introduction

Mild steel has low tensile strength compared to high-carbon steel but is easier to work with and more cost-effective. However, it is highly susceptible to corrosion, so protective measures such as painting, galvanizing, or corrosion inhibitors are often necessary. Therefore, corrosion of mild steel in acidic solutions is a critical area of study, particularly in various chemical processing industries such as oil well acidizing, petrochemicals, acid pickling, and acid descaling (Asmara *et al.*, 2018; Ghulamullah *et al.*, 2017). Corrosion is a prevalent phenomenon in oil and gas production, processing, and pipeline systems, occurring under diverse and complex conditions in almost any aquatic medium (Ibrahim *et al.*, 2020). The corrosion process involves three main components: an electrolyte, an anode, and a cathode. The cathode is an electrical conductor that remains intact during corrosion, while the anode is the corroding metal. The electrolyte facilitates electron transfer from the anode to the cathode (Abbas *et al.*, 2018).

Inhibitors are chemical substances used to protect metal surfaces in the oil and gas industries, preventing corrosion by interacting with the metal surface or reacting with environmental pollutants that cause damage (Ibrahim *et al.*, 2020; Abbas *et al.*, 2018; Zarrouk *et al.*, 2012). Corrosion inhibitors function in several ways: by blocking active sites on the metal surface, reducing the anodic or cathodic reaction rates; by promoting passivation through the formation of a natural oxide film; or by forming a protective thin layer on the metal surface (Hojatallah, 2019).

Numerous studies have reported the effectiveness of organic compounds as potent corrosion inhibitors for mild steel in acidic solutions (Beniken *et al.*, 2022; Musa *et al.*, 2013; Bouklah *et al.*, 2004). Organic inhibitors with heteroatoms such as oxygen, nitrogen, and sulfur, often combined with aromatic rings or π-electron systems, are particularly effective due to their high electron density (Ghulamullah *et al.*, 2017; Ghulamullah *et al.*, 2017). These organic inhibitors adsorb onto the metal surface, with their performance influenced by factors such as the type of electrolyte, metal composition, surface structure, and chemical properties (Abdulfatah *et al.*, 2013).

Schiff bases, which contain an azomethine functional group, are a notable class of organic corrosion inhibitors. They are widely favored for their cost-effective raw materials, straightforward synthesis, low toxicity, high purity, and environmental friendliness (Ma'rufah *et al.*, 2020). Studies have demonstrated that Schiff bases effectively inhibit the corrosion of metals such as mild steel, copper, zinc, and aluminum in aggressive environments (Beniken *et al.*, 2017; Ghulamullah *et al.*, 2017). These compounds adsorb on the metal surface, blocking active sites and protecting the metal from decomposition in corrosive solutions (Ghulamullah *et al.*, 2017).

This study aims to investigate the corrosion inhibition potential of 2-[2-(hydroxybenzylide)amino]benzanoic acid (SB1) and (2-hydroxybenzylidene)-(2-hydroxyphenyl) amine (SB2) Schiff bases on mild steel in 1M HCl solution using weight loss and potentiodynamic polarization techniques (PDP). The study also seeks to elucidate the mechanism of inhibition through the evaluation of the adsorption isotherms, kinetic and thermodynamic parameters.

2. Methodology

2.1 Synthesis of 2-[2-(hydroxybenzylide) amino] benzanoic acid Schiff base

The Schiff base, 2-aminobenzanoic acid was synthesized by dissolving (10.00 g, 7.29 mmol) in 50ml hot ethanol and 2-hydroxybenzaldehyde (6.08 ml, 7.29 mmol) in 50 ml hot absolute ethanol was added drop wise with stirring. The resulting solution was refluxed for 2hrs, an orange precipitate was formed overnight, filtered and washed with cold ethanol and allowed to dry in air. The product was recrystallized from hot ethanol and dried in a dissector (Ibrahim *et al.*, 2020)

2.2 Synthesis of (2-hydroxybenzylidene)-(2-hydroxyphenyl)-amine Schiff base

To synthesize the Schiff base, 2-hydroxybenzaldehyde (1.46 mL, 0.014 mol) was dissolved in absolute ethanol (20 mL) and added to an ethanolic solution (30 mL) of 2-aminophenol (1.5 g, 0.014 mol). The mixture was heated to reduce the volume to approximately 25 mL, and then cooled in an ice bath. The orange-red crystals formed were filtered, washed with cold ethanol, and air-dried. The product was recrystallized from hot ethanol and dried in a desiccator (Ibrahim *et al.*, 2020).

2.3 Preparation of specimen

The specimen (coupons) used for this research was mild steel with weight percentages as: C 0.21%, Si 0.38%, P 0.1%, S 0.04%, Mn 0.05%, Al 0.01% and Fe the rest. The mild steel was cut into 4 cm by 2.5 cm by 0.1 cm sizes dimensions. It was subjected to chemical treatments, degreased in absolute

ethanol and dried in acetone. All chemicals used in this study were of analytical grade quality, sourced from reputable suppliers.

2.4 Weight loss experiment

In this experiment, the coupons were weighed and completely immersed in 1M HCl solution, both in the absence and presence of varying inhibitor concentrations (0.1 to 0.4 mM). The solution was placed in an open beaker, covered with aluminum foil, and maintained in a water bath at 30°C for 1, 2, 3, and 4 hours. After immersion, the corrosion products were removed by washing each coupon with distilled water. The washed coupons were then rinsed with acetone, air-dried, and reweighed. The procedure was repeated at elevated temperatures of 40°C, 50°C, and 60°C, with an immersion time of 1 hour at each temperature. The weight loss (W_l), corrosion rate (CR), inhibition efficiency (I.E.), and surface coverage (θ) were calculated using equations (1–4), as described by Musa *et al.*, (2020); Siaka *et al.*, (2014):

$$\text{Weight loss } (\Delta W) = W_2 - W_1 \quad \text{Eqn. 1}$$

$$\text{CR (mg/cm}^2\text{h)} = \frac{\Delta W(mg)}{A(sq.cm) \times T(h)} \quad \text{Eqn. 2}$$

$$\text{I.E \%} = \left(1 - \frac{W1}{W2}\right) \times 100 \quad \text{Eqn. 3}$$

$$\Theta = 1 - \frac{W1}{W2}. \quad \text{Eqn. 4}$$

where W_1 and W_2 are the weight losses for the mild steel coupon in the presence and absence of inhibitor respectively, CR is the corrosion rate, A is the area of the mild steel coupon (cm^2), I.E is the inhibition efficiency, t is the time of immersion (in hour) and Θ is the surface coverage.

2.5 Potentiodynamic Polarization (PDP) Technique

The mild steel coupons were cut to 2.5cm by 4cm. The coupons were then submerged in a solution of 1M HCl at various concentrations of inhibitors (0.1mM to 0.4mM) for electrochemical studies. The experiments were conducted using three conventional electrode cells: a platinum foil served as the counter electrode, a saturated calomel electrode (SCE) served as the reference electrode, and the mild steel coupons as the working electrode. The experiments were carried out using an Autolabpotentiostat (PGSTAT 30 computer controlled) with an installed NOVA software version 1.8. The results were plotted as a graph of potential (E_{corr}) against current density (I_{corr}) using Origin software version 2020. The corrosion potential (E_{corr}) and corrosion current density (I_{corr}) were determined by extrapolating the linear Tafel regions of the anodic and cathodic curves. The inhibition efficiency (%I) was calculated using equation 5:

$$\%I = \frac{Icorr(0) - Icorr(inh)}{Icorr(0)} \times 100 \quad \text{Eqn. 5}$$

where $I_{corr(inh)}$ and $I_{corr(0)}$ are the corrosion current densities with and without the inhibitor (Ghulamullah *et al.*, 2017).

2.6 Fourier Transform Infra-Red Spectrophotometry (FT-IR)

The FT-IR spectra of the Schiff bases and the corrosion products (in the absence and presence of inhibitors) were carried out using a Fourier Transform Infrared Spectrophotometer. Each coupon was separately dipped in 100mL of 1.0 M (HCl) of acid-inhibitor concentration respectively for 4 days to form an adsorbed layer after which they were removed, dried, and scraped with a sharp razor blade for

analysis. The samples were prepared using KBr and the analysis was done through a wave number range of 4,000.00 – 650.00 cm^{-1} (Akalezi *et al.*, 2012).

2.7 Scanning electron microscopy (SEM)

Surface morphologies of the mild steel (coupons) in the absence and presence of inhibitors were studied using a Scanning electron microscope (JEOL JSM-7600F model). The coupons were immersed in 1M HCl solution in the absence and presence of 0.4mM inhibitor concentration at 300 K for 24 h. The mild steel samples were dried before placing them on the slide. The snapshots of the specimen were taken. Mild steel sample was investigated for their surface morphology.

3. Results and Discussion

3.1 Effect of time on Corrosion

Experimental analysis was used to study the effect of time on the corrosion control of mild steel using the prepared Schiff bases. The study was performed at a constant temperature of 303 K, with varying concentrations of the Schiff bases ranging from 0.1 mM to 0.4 mM, and over different time intervals from 1 hr to 4 hr. Figures 1a, 2a, and 3a for SB1 and Figures 1b, 2b, and 3b for SB2 illustrate the variations in weight loss, corrosion rate, and inhibition efficiency for time, respectively. Figures 1a and 1b, reveal that weight loss increases with increased immersion time. The results also indicated that the weight loss of mild steel was significantly lower in the presence of the Schiff bases inhibitor compared to the uninhibited system. This decrease in weight loss is attributed to the adsorption of the Schiff base onto the metal surface, which provides a protective barrier. Similar findings have been reported by other researchers (Ameh *et al.*, 2023; Musa *et al.*, 2013; Chetouani *et al.*, 2003).

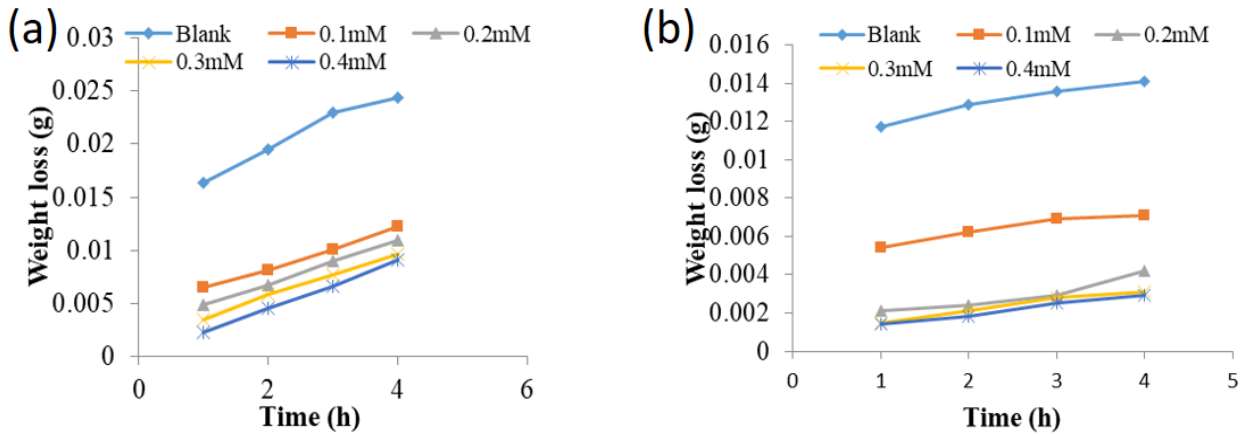

Figure 1. Variation of Weight loss with time for the corrosion of mild steel in 1.0 M HCl (a) in the absence and presence of different concentrations of SB1 at 303K and (b) in the absence and presence of different concentrations of SB2 at 303K

The corrosion rate and inhibition efficiency of mild steel in 1.0 M HCl at 303 K, determined using the weight loss method as a function of time in the presence of Schiff bases, are presented in Figures 2a, 2b and 3a, 3b, respectively for SB1 and SB2. Figure 2 (a and b) shows that the corrosion rate of mild steel coupons decreased with increasing inhibitor concentration. Meanwhile, Figure 3 (a and b) demonstrates that inhibition efficiency decreased with prolonged immersion time. These results are consistent with those reported by Musa *et al.* (2013) & Arrousse *et al.*, (2021).

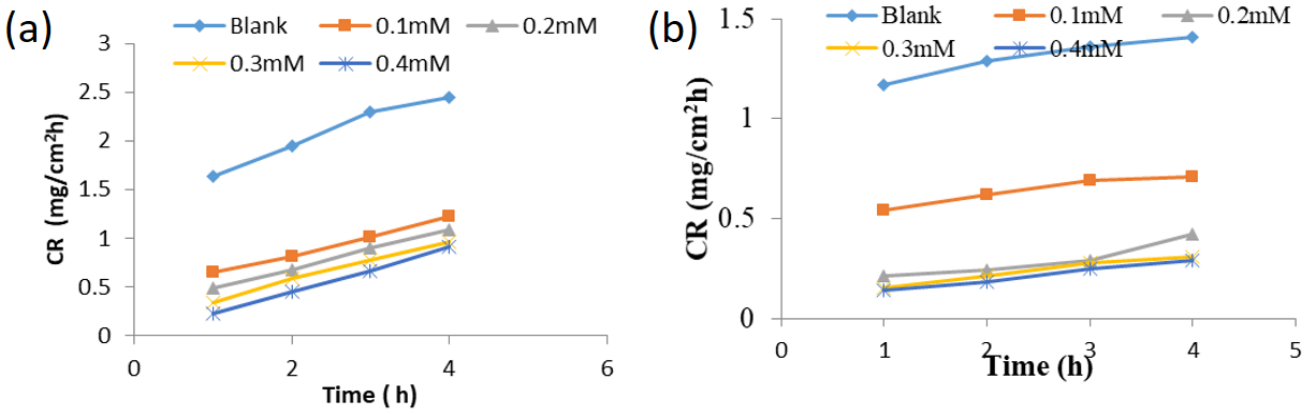

Figure 2. Effect of immersion time on the corrosion rates of mild steel in 1.0 M HCl (a) in the absence and presence of SB1 and (b) in the absence and presence of SB2

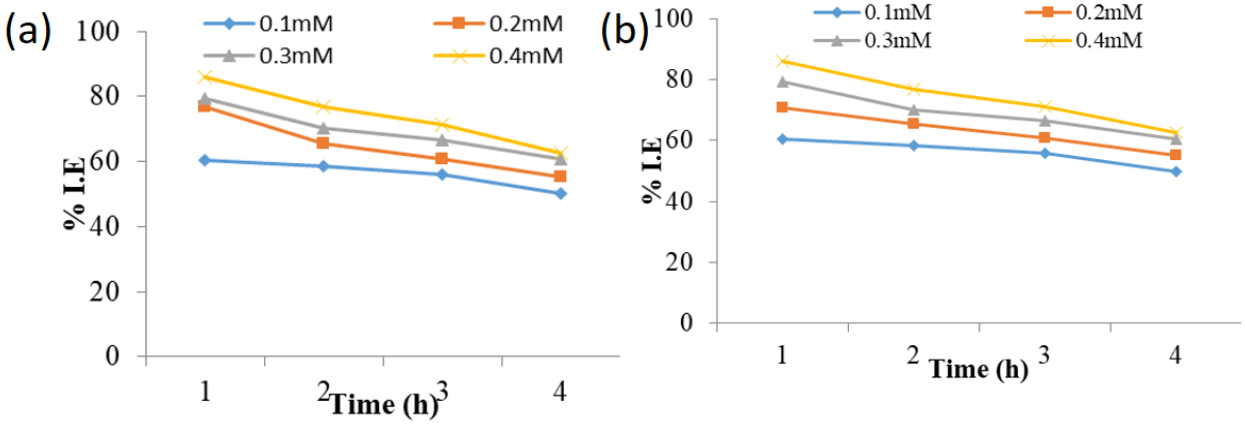

Figure 3. Effect of Immersion Time (h) on Corrosion Inhibition Efficiency (%IE) of mild steel in 1.0 M HCl (a) in the presence of various concentrations of SB1 and (b) in the presence of various concentrations of SB2

3.2 Effect of Temperature

Figures 4a and 4 b show the effect of temperature on the weight loss of mild steel in the absence and presence of Schiff base on 1M HCl solution for SB1 and SB2, respectively.

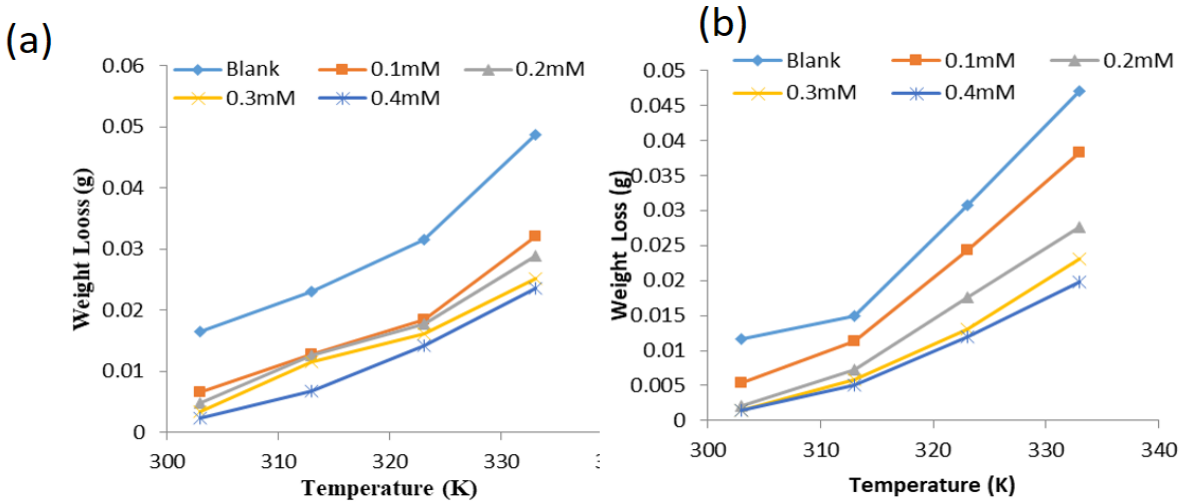

Figure 4. Variation of weight loss with temperature for the corrosion of mild steel (a) in absence and presence of SB1 in 1M HCl and (b) in the absence and presence of SB2 in 1M HCl

Figure 4 (a and b) illustrates the variation of weight loss in mild steel at different temperatures. Weight loss increases with temperature increase due to the reaction's higher kinetic energy, which increases the corrosion rate. However, the weight loss decreases as the concentration of the Schiff bases increases, even at elevated temperatures. Also, the weight loss, corrosion rate, surface coverage, and inhibition efficiency for various concentrations of SB1 and SB2 in 1M HCl are presented in Figures 4a and 4b at different temperatures respectively. It can be seen that the corrosion rate increases with an increase in temperature, while the inhibition efficiency gradually decreases. This indicates that, although the Schiff bases effectively retard the dissolution of mild steel, its efficiency diminishes at higher temperatures. The reduction in inhibition efficiency is attributed to the increased mobility of inhibitor molecules at elevated temperatures, which reduces their interaction with the metal surface. Additionally, the rate of chemical reaction increases with an increase in temperature, so this increase in temperature leads to faster etching as well as desorption of adsorbed Schiff base from mild steel surface (Frederich *et al.*, 2020; Jeyaprabha and Bhuvaneswari, 2022).

3.3 Effect of inhibitor concentration

The effect of inhibitor concentrations on the corrosion rate of mild steel in 1M HCl is shown in Figures 5a and 5b. The results indicated that inhibited systems exhibit lower corrosion rates than uninhibited systems. Temperature variations between 303 K and 333 K were used to study the corrosion rate. The findings reveal that for all the tested temperatures, the corrosion rate of mild steel in 1M HCl decreases as the inhibitor concentration increases. This is attributed to the enhanced adsorption of inhibitor molecules onto the mild steel surface with increasing concentration, forming a protective barrier that impedes charge and mass transfer. Consequently, the interaction between the mild steel surface and the corrosive medium is reduced, slowing down the corrosion rate. These results align with the findings of Musa *et al.* (2019).

Figures 6a and 6b illustrate the effect of inhibitor concentration on inhibition efficiency for SB1 and SB2 respectively. The results showed that as the inhibitor concentration increases, the inhibition efficiency also improves. This is due to more of the inhibitor's molecules adsorbing onto the mild steel surface, covering a larger area and providing more effective protection. Up to a concentration of 0.4 mM, the inhibition efficiency increases significantly, consistent with the findings of Musa *et al.* (2020) & Kalkhambkar *et al.* (2022).

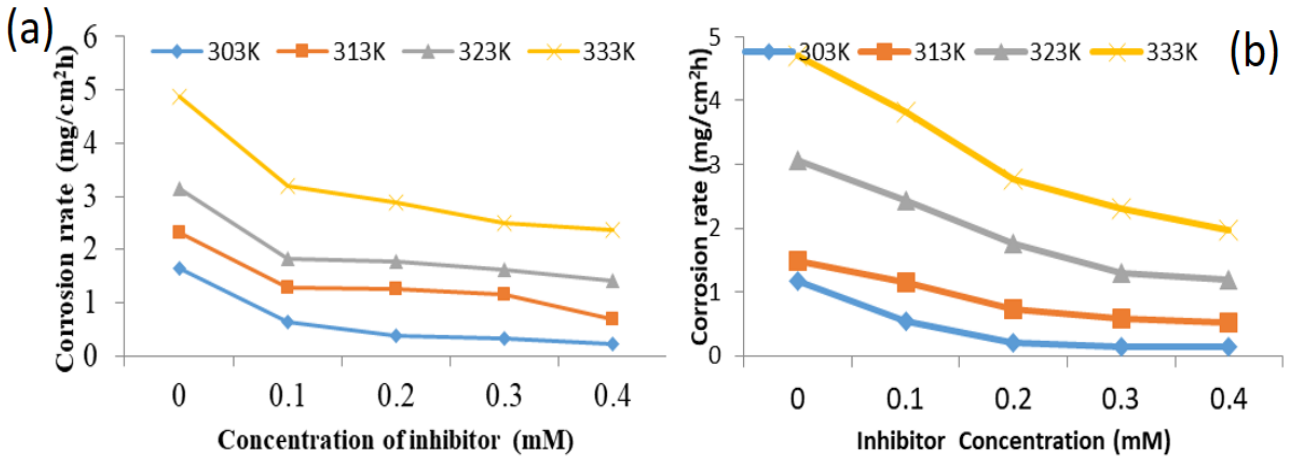

Figure 5. Variation of Corrosion Rate with Inhibitor Concentration of (a) SB1 for mild steel corrosion in HCl and (b) SB2 for mild steel corrosion in HCl.

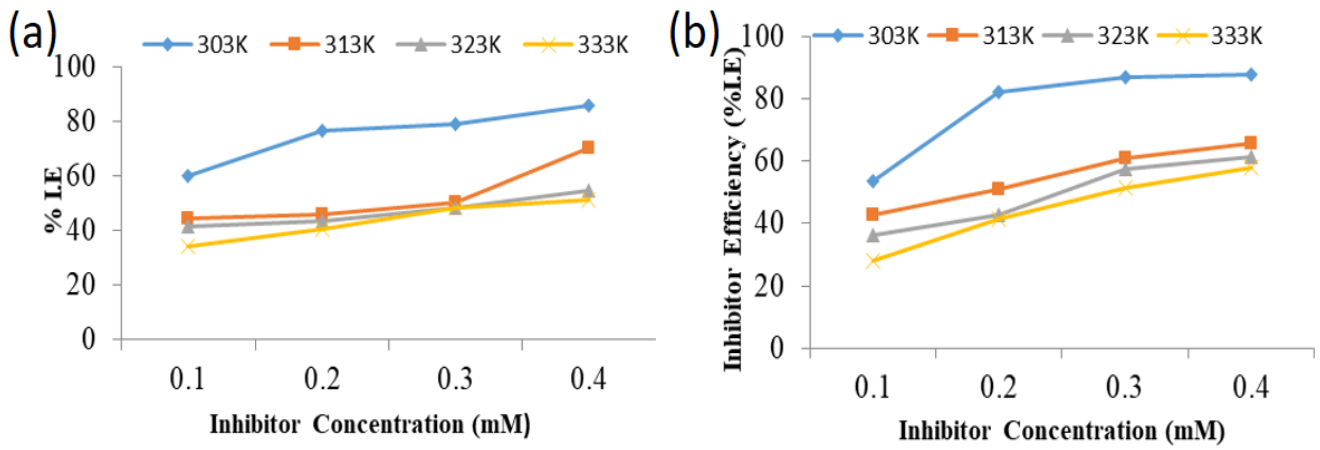

Figure 6. Variation of Inhibition Efficiency with Inhibitor Concentration of (a) SB1 for mild steel corrosion in HCl and (b) SB2 for mild steel corrosion in HCl.

3.4 Adsorption consideration

To comprehend the relationship between the inhibitor and the mild steel surface, some selected adsorption isotherms were utilized. To determine which isotherm best fits the data, the degree of surface coverage (Θ) obtained from the weight loss experiments was employed. The Langmuir, Freundlich and Temkin isotherms were utilized to determine the optimal isotherms based on the experimental data. To identify which model best fits the generated data, R2 values closer to unity where adjudged fitting the model equation. Out of the isotherms studied, the Langmuir adsorption isotherm was proved to fit best the data generated for both Schiff bases as inhibitor. The equation 6 can be used to express the Langmuir adsorption isotherm.

$$\frac{Cinh}{\theta} = \frac{1}{Kads} + C_{inh} \qquad \text{Eqn. 6}$$

where K_{ads} is the adsorption equilibrium constant, surface coverage (Θ) and C_{inh} is the concentration of inhibitor. A graph of $\frac{Cinh}{\theta}$ against C_{inh} was plotted as showed in figure 7a and 7b for SB1 and SB2 respectively. At every temperature, straight lines with R^2 value nearly close to unit were obtained. This shows that the Schiff bases' adsorption followed the Langmuir adsorption isotherm at temperature of 303 K to 333 K.

Additionally, it suggests that the Schiff bases occur at common adsorption sites at the metal/solution interface. Adsorption isotherm parameters obtained from different isotherms are presented in Tables 1 and 2, as the temperature increased from 303 K to 333 K, the adsorption equilibrium constant (K_{ads}) decreased. Since the magnitude of the adsorption constant (K_{ads}) determines an inhibitor's efficiency, large value of K_{ads} suggest a stronger and better contact between the inhibitor molecules and the mild steel, whereas small values of K_{ads} indicate a weaker interaction. The value of the adsorption equilibrium constant (K_{ads}) obtained at 303K is higher compared to the values obtained at 313K, 323K and 333K. This implies that Schiff bases was more efficient as an inhibitor at 303K compared to the other temperatures (313 K, 323 K and 333 K) (Evelyn *et al.*, 2017). The results obtained in this research work are inline with work of other reported researches (Ameh *et al.*, 2023; Hsissou *et al*, 2022; Chahul *et al.*, 2015).

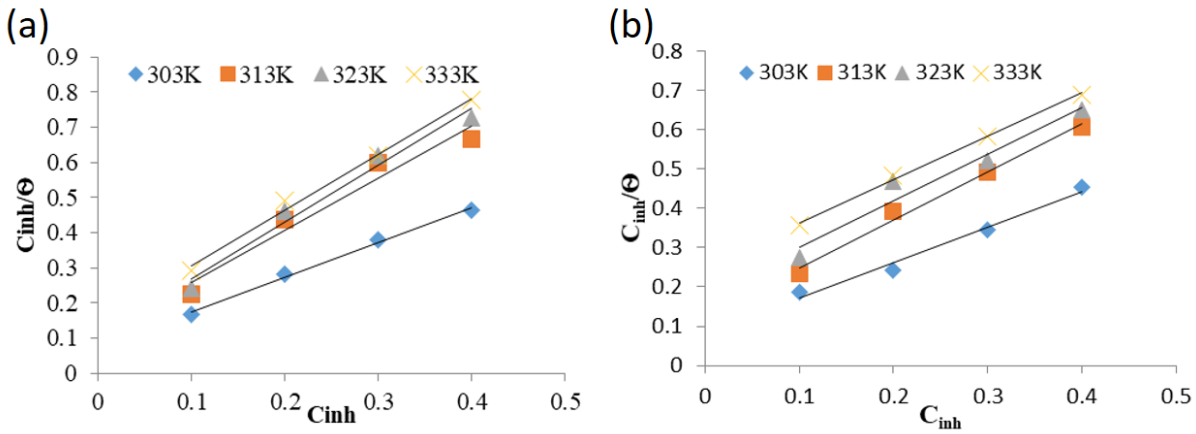

Figure 7. Langmuir adsorption plots for the corrosion of mild steel in 1M HCl solution (a) in the presence of the SB1 at different temperature and (b) in the presence of the SB2 at different temperature

Table 1. Adsorption parameters for the adsorption of SB1 on mild steel surface

Isotherm	Temperature (K)	Slope	K_{ads} ×10^3	ΔG_{ads} (kJ/mol)	R^2
Langmuir	303	0.991	13.333	-34.045	0.995
	313	1.489	9.259	-34.222	0.955
	323	1.489	9.174	-34.291	0.977
	333	1.583	6.757	-35.537	0.993
Freundlich	303	0.254	1.086	-27.731	0.952
	313	0.281	0.794	-27.830	0.641
	323	0.191	0.625	-28.078	0.855
	333	0.303	0.684	-29.195	0.987
Temkin	303	0.183	1.017	-27.565	0.988
	313	0.156	0.763	-27.727	0.606
	323	0.090	0.608	-28.003	0.833
	333	0.127	0.630	-28.968	0.979

3.5 Free Energy of Adsorption

Equations 7 and 8 relates the adsorption equilibrium constant (K_{ads}) to the adsorption free energy (ΔG_{ads}):

$$K_{ads} = \frac{1}{55}\exp\left(\frac{-\Delta Gads}{RT}\right) \quad \text{Eqn. 7}$$

This can be writing as:

$$\Delta G_{ads} = -RT\ln(55.5K_{ads}) \quad \text{Eqn. 8}$$

where R is the universal gas constant, T is the temperature, the constant value 55.5 is the concentration of water and K_{ads} is the adsorption equilibrium constant.

Absolute values of ΔG_{ads} up to 20 kJ/mol often correspond to physisorption, whereas those around -40 kJ/mol or greater are associated with chemisorptions. This results from the sharing or transfer of electron from organic molecules to the metal surface, which forms a specific types of coordinate metal bond (Paul *et al.*, 2012). From the result obtained, the calculated values of ΔG_{ads} for all three tested isotherms presented in Tables 2 and 3 are less than the threshold value of -40 kJ/mol and are all negative. This implies that the adsorption of the inhibitor molecules on the mild steel surface occurs

spontaneously, as indicated by the negative values of ΔG_{ads} (Musa *et al.*, 2020). The calculated ΔG_{ads} values for Langmuir isotherm range from -34.045 to -35.537 kJ/mol and -33.854 to -34.063 kJ/mol for SB1 and SB2 respectively, indicating that the adsorption of Schiff bases is ionic electrostatic adsorption (physisorption) on mild steel in a 1M HCl solution at the temperatures taken into consideration, nevertheless, these values are around the chemisorptions threshold, indicating that the adsorption process can continue via a combination of chemisorptions and physisorption modes. Adsorption behavior like this is a common adsorption mode for organic molecules with heteroatom-based functional groups and Π-bonding electrons (Fatemeh *et al.*, 2012). These molecules might interact with the surface of the metal through electrostatic interaction that can cause chemisorptions as well as electron transfer between the organic inhibitor and the metal surface. The results obtained in this study agreed with the results reported by some researchers (Musa *et al.*, 2020; Chahul *et al.*, 2015).

Table 2. Adsorption parameters for the adsorption of SB2 on mild steel surface

Isotherm	Temperature (K)	Slope	$K_{ads} \times 10^3$	ΔG_{ads} (kJ/mol)	R^2
Langmuir	303	0.904	12.346	-33.854	0.982
	313	1.218	7.874	-33.801	0.990
	323	1.179	5.435	-33.885	0.955
	333	1.104	3.968	-34.063	0.997
Freundlich	303	0.366	0.324	-28.229	0.870
	313	0.321	0.883	-28.106	0.987
	323	0.402	0.889	-29.023	0.944
	333	0.507	0.980	-30.191	0.873
Temkin	303	0.253	1.160	-27.896	0.889
	313	0.310	0.971	-28.354	0.972
	323	0.303	0.913	-29.095	0.986
	333	0.282	0.849	-29.794	0.993

3.6 Thermodynamics study

The activation energy of the corrosion of mild steel coupons in 1.0M HCl in the absence and presence of Schiff base was evaluate using the values of the corrosion rates of the mild steel at different temperature. Using the Arrhenius equation, the activation energy can be deduced according to equation 9 by Jeyaprabha and Bhuvaneswari (2022).

$$ln(CR) = lnA - \frac{Ea}{RT} \qquad \text{Eqn. 9}$$

where A is Arrhenius pre-exponential factor, CR is the rate of corrosion, T is the absolute temperature in Kelvin, and R is the universal gas constant.

From the Arrhenius plot of ln CR against $\frac{1}{T}$ gave a straight line with slope equal to –Ea/R from which the value of the activation energy (E_a) at different temperatures were calculated and presented in Table 3. The values obtained for the activation energy in the presence of inhibitors are higher than in the absence of inhibitors, this indicates that the Schiff bases retarded the corrosion of the mild steel in 1.0M HCl and this might be due to the uniform adsorption of the Schiff bases on the surface of the metal

thereby lowering the corrosion rates. However, the activation energy value of 80 kJ/mol or greater is required for chemisorption and an activation energy value < 80 kJ/mol indicates physisorption, and in this study the activation energy range from 29.72 to 64.19kJ/mol and 40.73 to 76.83kJ/mol for SB1 and SB2 respectively which suggest physical adsorption of Schiff base on the mild steel surface. This finding corresponds with the results reported by Abdulilah *et al.* (2023).

Table 3. Adsorption parameters for the adsorption of SB2 on mild steel surface

Inhibitor	Concentration (mM)	E_a (kJ/mol)	ΔH_a (kJ/mol)	ΔS_a ($kJK^{-1}mol^{-1}$)
SB1	Blank	29.723	27.112	0.1516
	0.1	42.768	40.14	0.1157
	0.2	47.607	45.03	0.1013
	0.3	52.712	50.05	0.08688
	0.4	64.193	61.58	0.0528
SB2	Blank	40.73	38.13	0.1186
	0.1	54.98	49.44	0.08638
	0.2	71.54	68.95	0.02893
	0.3	74.80	72.18	0.02087
	0.4	76.83	70.50	0.02710

3.7 Enthalpy of activation (ΔH) and Entropy of activation (ΔS):

Enthalpy of activation (ΔH) and Entropy of activation (ΔS) can be calculated using the transition state equation (10) given according to Abbas *et al.* (2018).

$$\ln\frac{CR}{T} = [\ln(\frac{R}{hN}) + (\frac{\Delta S}{R})] - \frac{\Delta H}{RT} \qquad \text{Eqn. 10}$$

Where CR is the corrosion rate, N is Avogadro's number, T is absolute temperature, R is the universal gas constant and h is Planck's constant.

Plot of lnCR/T against 1/T gives a straight line graph with slope equal to $-\Delta H_a/R$ and intercept equal to $[\ln(R/hN) + (\Delta S_a/T)]$ from which the enthalpy of activation and entropy of activation were calculated and presented in Table 3. From the result obtained, it can be seen that the enthalpies (ΔH_a) values are all positive and increases with increase in concentration of inhibitor thus reflect the endothermic nature of the mild steel dissolution process and adsorption heat increases with increasing in concentration of inhibitor (Eddy *et al.*, 2011). The entropy changes of activation values are negative and decrease with increase in concentration of the inhibitor, this implies that there is an association rather than dissociation in the activated complex of the rate determining step, indicating that a decrease in disorder take place, going from reactant to the activated complex.

It's important to show that the difference $E_a - \Delta H_a = 2.6$ kJ/mol with is in good agreement with the relation $E_a - \Delta H_a = RT$ at 318K (mean temperature (303-333) K. This result confirms that the reaction of hydrogen ion reduction toward hydrogen atom (monoatomic molecule) is principal (Ghenimi *et al.*, 2024; Khadim *et al.*, 2021; Nahlé *et al.*, 2021).

3.8 Potentiodynamic Polarization

Tables 4a and 4b display electrochemical parameters for mild steel metal corrosion in 1M HCl solution with different concentrations of SB1 and SB2 that were derived from the Tafel plot and figure 8a and 8b shows the plot obtained from Potentiodynamic polarization study for the uninhibited and inhibited mild steel corrosion system.

Table 4a. Electrochemical characteristics for mild steel corrosion in 1 M HCl solution at different concentrations of SB1

Inhibitor Concentration (mM)	i_{corr} ($mAcm^{-2}$)	E_{corr} (mV)	β_a ($mVdec^{-1}$)	β_c ($mVdec^{-1}$)	C.R ($mmpy^{-1}$)	%I
0.0	8.63	-565.97	185.70	46 0.47	4.77	-
0.1	6.16	-569.62	168.10	371.10	3.41	28.58
0.2	2.85	-558.53	112.80	209.60	1.58	66.92
0.3	2.21	-566.92	98.90	130.40	1.22	74.38
0.4	1.82	-563.31	65.60	105.90	1.01	78.86

Table 4b. Electrochemical characteristics for mild steel corrosion in 1 M HCl solution at different concentration of SB2

Inhibitor Concentration (mM)	i_{corr} ($mAcm^{-2}$)	E_{corr} (mV)	β_a ($mVdec^{-1}$)	β_c ($mVdec^{-1}$)	C.R ($mmpy^{-1}$)	% I
0.0	8. 63	-565.97	185.70	460.47	4.77	-
0.1	5.93	-566.13	134.40	250.20	3.23	31.24
0.2	3.39	-556.51	135.00	169.50	1.87	60.75
0.3	3 .08	-564.40	103.60	139.60	1.70	64.28
0.4	1.97	-557.86	96.60	150. 50	1.09	77.15

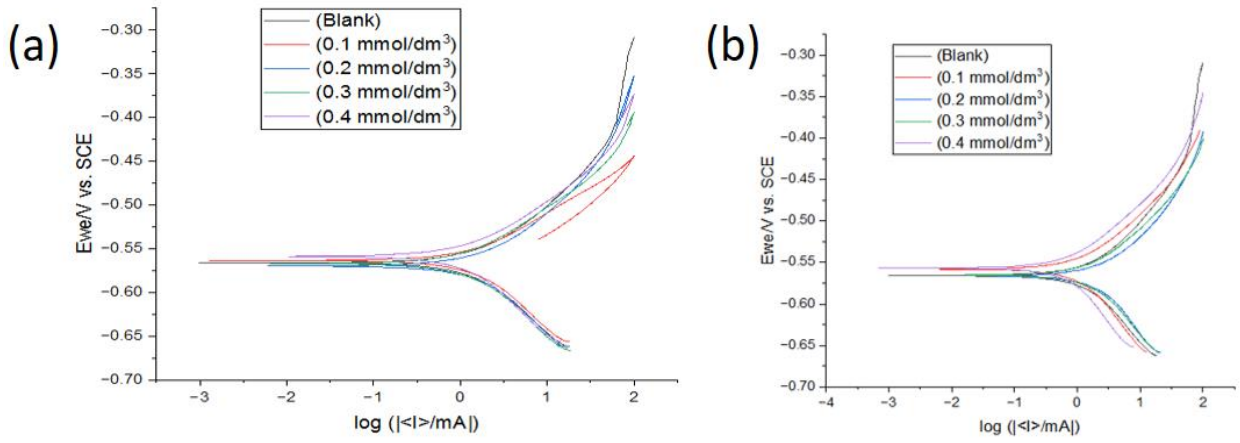

Figure 8. Tafel plot of the mild steel in the absence and presence of (a) SB1 and (b) SB2

The Anodic and cathodic plots were recorded on a mild steel electrode in 1M HCl without and with varying concentrations of Schiff bases at room temperature (Figure 8 a and b). According to the intersection of the anodic and cathodic Tafel lines, the associated electrochemical parameters, such as

corrosion potential (E_{corr}), corrosion current density (I_{corr}), anodic and cathodic Tafel constant (β_a and β_c) and corrosion inhibition efficiencies (%I), were calculated and showed in Table 4. It is evident from Figure 8a and 8b and Table 4a and 4b that the anodic and cathodic portions of the Tafel slopes were impacted by the addition of Schiff bases to the acid media. When inhibitor molecule is added to an acidic media, the corrosion current density (I_{corr}) is reduced. Stated otherwise, there is significant inhibition of both anodic metal dissolution and cathodic reaction stop reducing hydrogen gas. This behavior suggested that when the concentration of the inhibitor increases, it may suppress the production of hydrogen gas through both the cathodic process and the anodic metal dissolution. Additionally, Table 4 shows that while inhibition efficiencies rise as predicted, from 28.58, 66.92, 74.38 and 78.86% for SB1 and 31.24, 60.75, 64.28 and 77.15% for SB2 at 0.1, 0.2, 0.3 and 0.4mM respectively and corrosion current densities fall as inhibitor concentration rise.

3.9 Surface Morphology

The morphology of the mild steel surface was analyzed and correlated with the experimental parameters using SEM imaging. Figures 9 (c and d) shows images of the mild steel surface in the presence of 0.4 mM of SB1 and SB2, while Figure 9 (a, b) shows the surface image of the abraded sample before and after immersion in a 1 M acid solution for 24 hours. Figure 9b shows that the surface region has obvious pitting and cracking evidence as a result of aggressive solution attaches in the absence of inhibitors and corrosion product production. The mild steel surface photomicrograph (Figure 9 (c, d)) in the presence of inhibitors shows a rather smooth surface with few pits or cracks. These findings show that the presence of Schiff base inhibitor (SB1 and SB2) prevents mild steel from dissolving because the inhibitor molecules adsorb onto the surface and form a layer of protection, which lowers the mild steel's dissolution rate in 1M HCl solution.

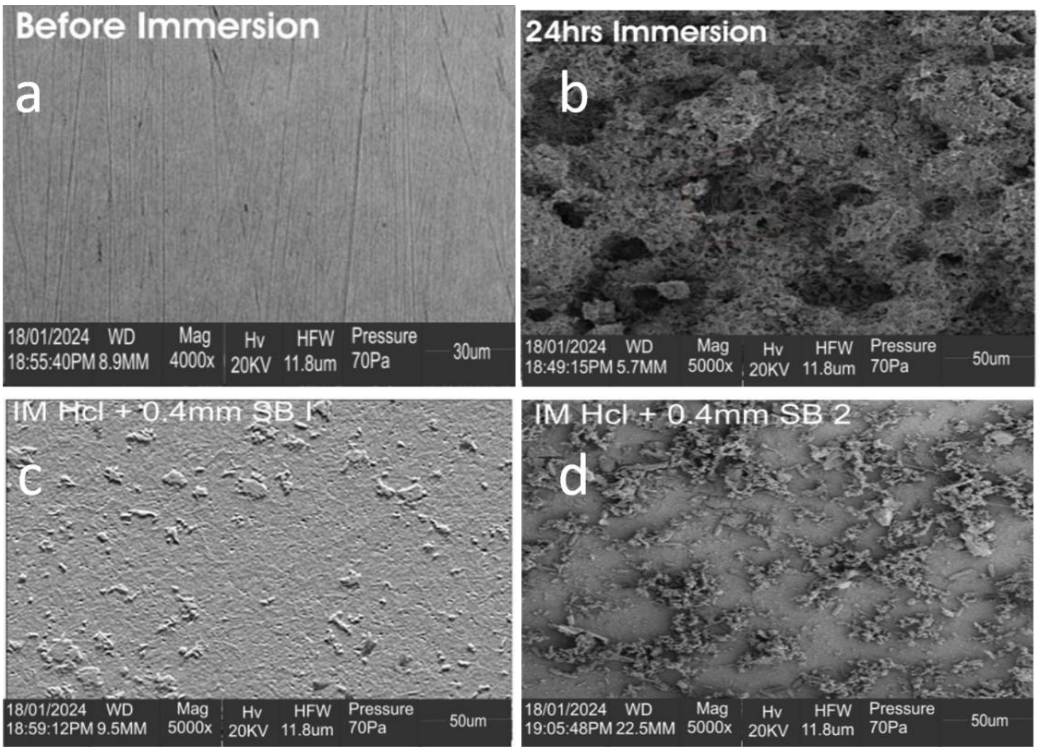

Figure 9. SEM micrographs of mild steel surface after immersion in 1M HCl for 24hours at room temperature: (a) Polished Mild Steel surface; (b) Mild steel immersed in 1M HCl (c) immersion in 1M HCl containing 0.4mM SB1 inhibitor; (d) immersion in 1M HCl containing 0.4mM SB1 inhibitor

Fourier Transform Infra-red Spectroscopy

The FTIR spectra of the synthesized Schiff bases and the corrosion product are shown in Figure 10 (a,b, c and d). FTIR spectroscopy was utilized to provide addition evidence for inhibitor's adsorption behavior on the mild steel surface. The FTIR spectra of inhibitors (SB1 and SB2) were displayed in Figure 10a and figure 10c respectively. The spectra of the corrosion product when SB1 and SB2 were used as inhibitors respectively are displayed in figure 10b and figure 10d. For SB1, comparing figure 10a and figure 10b it also evident that the C-O stretch at 1361cm^{-1} was shifted to 1246 cm^{-1}, the O-H at 3368 cm^{-1} was shifted to 3327 cm^{-1}, the C=C from aromatic ring at 1678 cm^{-1} was shifted to 1760 cm^{-1}, the C-H aromatic ring at 3037 cm^{-1} was shifted to 3152 cm^{-1} and the C=N at 1618 cm^{-1} was shifted to 1547 cm^{-1}. However, it can be seen clear that some peak in figure 10b were shifted in figure 10d, this include, the O-H at 3551cm^{-1} was shifted to 3394cm^{-1}, the C-H of aromatic ring at 3044cm^{-1} was shifted to 3001cm^{-1}, the C=C of aromatic ring at 1614cm^{-1} was shifted to 1559cm^{-1}, the C=N at 1592cm^{-1} was shifted to 1544cm^{-1}, the C-O stretch at 1413cm^{-1} was shifted to 1491cm^{-1}. These shifts in frequencies implies that there is an interaction between the Schiff bases with mild steel surface (Ibrahim *et al.*, 2020). Therefore SB1 and SB2 was adsorbed onto the surface of mild steel through functional group and pi-electron.

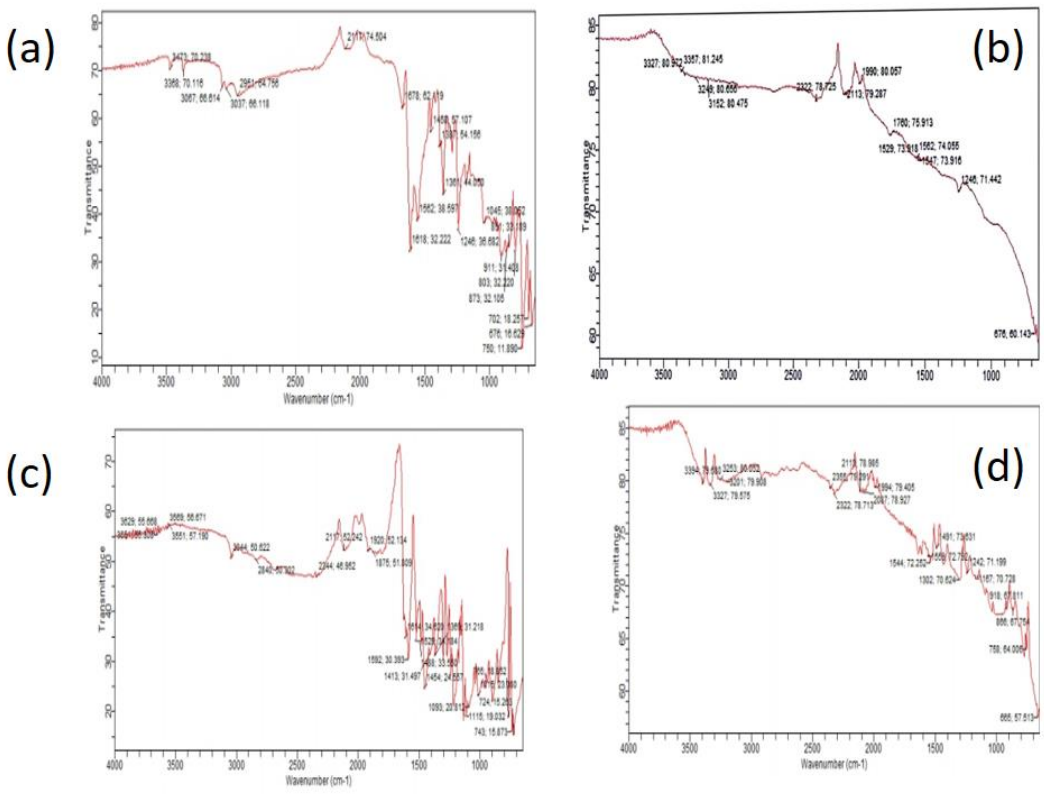

Figure 10. FTIR spectrum of (a) SB1, (b) Corrosion product of mild steel in 1M HCl medium with 0.3 mM SB1, (c) SB2 and (d) Corrosion product of mild steel in 1M HCl medium with 0.3 mM SB2

Conclusion

The Schiff bases were successfully synthesized and characterized using FTIR spectroscopy. They demonstrated effective corrosion inhibition for mild steel in a 1M HCl medium, achieving inhibition efficiencies of 89.98% and 88.03% at a concentration of 0.4 mM for SB1 and SB2, respectively. The corrosion inhibition efficiency increased with inhibitor concentration and decreased with rising

temperature. Polarization studies revealed that the inhibitors act as anodic-type inhibitors. The adsorption of Schiff bases on the mild steel surface in 1M HCl followed the Langmuir adsorption isotherm, indicating chemical adsorption. The positive enthalpy change of activation (ΔH_{ad}) in both blank and inhibited acid solutions confirmed the endothermic nature of the process. Additionally, the negative values of ΔG_{ads} indicated the spontaneity of the adsorption process. SEM analysis revealed that the mild steel surface was protected by adsorption films, and FTIR results confirmed that inhibition occurred through the adsorption of functional groups and aromatic rings present in the Schiff bases.

Acknowledgement: The laboratory space provided by the Advanced Corrosion and Electrochemical Research group of the Pure and Industrial Chemistry, Bayero University Kano is acknowledged.

Disclosure statement: *Conflict of Interest:* The authors declare that there are no conflicts of interest.
Compliance with Ethical Standards: This article does not contain any studies involving human or animal subjects.

References

Abbas A.S., E. Fazakas and T.I. Torok (2018) Corrosion studies of steel rebar samples in neutral sodium chloride solution also in the presence of a bio-based (green) inhibitor. *Int. J. Corros. Scale Inhib.*, 7(1) , 38 - 47.

Abdulfaatai A. Siaka, N. O. Eddy, S. O. Idris, L. Magaji, Z. N. Garba, I. S. Shabanda (2013) Quantum Chemical Studies of Corrosion Inhibition and Adsoption Potentials of Amoxicillin on Mild Steel in HCl Solution. *International Journal of Modern Chemistry,* 4(1) , 1-10.

Abdulilah Dawoud Bani-Yaseen, M. S.-L. (2023) Experimental and Theoretical Investigations of the effect of Bis-phenylurea-Based Aliphatic Amine Derivative as an Efficient Green Corrosion Inhibitor for carbon Steel in HCl Solution. *Journal Pre-proof* , 1-34.

Akalezi C. O., Enenebaku C. K and Oguzie E. E. (2012) Application f aqueous extracts of coffee senna for control of mild steel corrosion on acidic environments. International *Journal of Industrial Chemistry,* 3, 13 - 25.

Ali Kadhim Al-Edan, Wan Nor Roslam Wan Isahak, Zatil Amali Che Ramli, Waleed Khalid Al-Azzawi, Abdul Amir H. Kadhum, Hazim Saad Jabbar Ahmed Al-Amiery (2023) Palmitic acid-based amide as a corrosion inhibitor for mild steel in 1M HCl. *Heliyon,* 9(4).

Ameh O. M., Chahul H. F., Ike D. C. (2023) Evaluation of th Adsorption and Corrosion Inhbition Effects of Piliostigma thhonningii Extract on Mild Steel in 1.0 M Hydrochloric Acid. *J. Mater. Environ. Sci,* 14 (01) 97-112.

Arrousse N., Salim R., Abdellaoui A., et al. (2021), Synthesis, characterization, and evaluation of xanthene derivative as highly effective, nontoxic corrosion inhibitor for mild steel immersed in 1 M HCl solution, *Journal of the Taiwan Institute of Chemical Engineers,* 120, 344-359, https://doi.org/10.1016/j.jtice.2021.03.026

Asmara Y.P., Kurniawan T., Edy Sutjipto A.G., Jamiluddin J. (2018) Application of Plants Extracts as Green Corrosion Inhibitors for Steel in Concrete. *Indonesian Journal of Science & Technology*, 3 (2), 158 - 170.

Ayuba Abdullahi Muhammad, Nyijime Aondofa Thomas, Safiyya Abubakar Minjibir, Najib Usman Shehu, Fater Iohuna (2023) Exploring the Inhibition Potential of Carbamodithionic acid on Fe (111) Surface: A Theoretical Study. *Journal of Engineering in Industrial Research,* 4(4) , 201-210.

Beniken M., Salim R., Ech-Chihbi E., et al. (2022), Adsorption behavior and corrosion inhibition mechanism of a polyacrylamide on C–steel in 0.5 M H_2SO_4: Electrochemical assessments and molecular dynamic simulation, *Journal of Molecular Liquids*, 348, 118022, doi.org/10.1016/j.molliq.2021.118022

Bouklah M., Hammouti B., Aouniti A., Benhadda T. (2004) Thiophene derivatives as effective inhibitors for the corrosion of steel in 0.5M H2SO4. *Prop. Org. Coat.* 49N°3, 225-228, https://doi.org/10.1016/j.porgcoat.2003.09.014

Chahul H. F., Ayuba A. M., and Nyior S. (2015) Adsorptive, Kinetic, Thermodynamic and Inhibitive Properties of Cissus Populnea Stem Extract on the Corrosion of Aluminium in Acid Medium. *ChemSearch Journal* 6(1) , 20-30.

Chetouani A., K. Medjahed, K. E. Benabadji, et al. (2003). Poly (4-vinylpyridine isopentyl bromide) as inhibitor for corrosion of pure iron in molar sulphuric acid, *Prog. Org. Coat.* 46 N°6, 312-316, https://doi.org/10.1016/S0300-9440(03)00019-5

Eddy O. Nnabuk, Femi E. Awe, Abdulfatai A. Siaka, Ladan Magaji, Eno E. Ebenso (2011) Chemical Information From GC-MS Studies of Ethanol Extract of Andrographis Paniculation and Their Corrosion Inhibition Potentials on Mild Steel in HCl Solution. *International Journal of Electrochemical Science* 6 , 4316 - 4328.

Evelyn U. Godwin-Nwakwasi, Elachi E. Elachi, Mercy A. Ezeokonkwo, Lawrence E. Onwuchuruba (2017) A Study of the Corrosion Inhibition of Mild Steel in 0.5M Tetraoxosulphate (VI) acid by Alstonia boonei Leaves Extract as an Inhibitor at different temperatures. *International Journal of Advanced Engineering, Management and Science (IJAEMS)*, 3(12), 1150 - 1157.

Fatemeh Baghaei Ravari, Athareh Dadgarineshad (2012) New Synthesized Schiff base as Inhibitor of Mild Steel Corrosion in Acid Medium. *Gazi University Journal of Science*, 25(4), 835 - 842.

Frederick Okhakumhe Oshomogho, Thelma Ejiro Akhihiero, Osariemen Edonkpayi, and Joy Ehimwenma Ossai (2020) Green Corrosion Inhibition of Mild Steel using Prunus dulcis Seeds Extract in an Acidic Medium. *Global Journal of Pure and Applied Sciences*, 26, 171-178.

Ghenimi G., Ouakki M., Ferraa N., Barebita H., Guedira T., Cherkaoui M. (2025) Elaboration and investigation of corrosion inhibition by bismuth glasses for mild steel in 1.0 M HCl solution, *Mor. J. Chem.*, 13(1), 440-458, https://doi.org/10.48317/IMIST.PRSM/morjchem-v13i1.53043

Ghulamullah Khan, Wan Jeffrey Basirun, Salim Nwaz Kazi, Pervaiz Ahmed, Ladan Magaji, Syed Muzamil Ahmed, Ghulan Mustafa Khan, Muhammad Abdur Rehman (2017) Electrochemical investigation on the corrosion inhibition of mild steel by Quinazoline Schiff base compounds in hydrochloric acid solution. *Journal of Colloid and Interface Science*, 502, 135-145.

Hojatallah Koraee, H. E. (2019) Thermodynamic and Kinetic Investigation of Corrosion Inhibition Behavior of 2-MBT on Steel at a pH of 8. *Iranian Journal of Oil & Gas Science and Technology*, 8(3), 101 - 112.

Hsissou R., Benhiba F., El Aboubi M., About S., *et al.* (2022), Synthesis and performance of two ecofriendly epoxy resins as a highly efficient corrosion inhibition for carbon steel in 1 M HCl solution: DFT, RDF, FFV and MD approaches, *Chemical Physics Letters*, 806, 139995, ISSN 0009-2614, https://doi.org/10.1016/j.cplett.2022.139995

Ibrahim I.A., Mahmud S.D., Sani S. and Almustapha M.N. (2020) Synthesis of Schiff base Derived from Anthranilic acid and its Potentials on oil and gas Pipeline Corrosion Inhibition. *Nigerian Research Journal of Chemical Sciences*, 8(2), 57 - 65.

Jeyaprabha C. and Bhuvaneswari (2022) Thermodynamics, Adsorption and Spectral Studies of the Corrosion Inhibition of Mild Steel by Different Leaf Extracts in 1.0N HCl: Comparative Analysis. *Journal of University of Shanghai for Science and Technology* 24(10), 128 - 144.

Kalkhambkar A.G., Rajappa S.K. (2022), Effect of Schiff's bases on corrosion protection of mild steel in hydrochloric acid medium: Electrochemical, quantum chemical and surface characterization studies, *Chemical Engineering Journal Advances*, 12, 100407, ISSN 2666-8211, https://doi.org/10.1016/j.ceja.2022.100407

Kadhim A., Betti N., Al-Bahrani H. A., Al-Ghezi M. K. S., Gaaz T., Kadhum A. H. and AlamieryA. (2021) A mini review on corrosion, inhibitors and mechanism types of mild steel inhibition in an acidic environment, *Int. J. Corros. Scale Inhib.*, 10(3), 861-884

Ma'rufah L., Ahmad Hanapi A., Ningsih R., A. Ghanaim Fasya (2020) Synthesis of Schiff Base Compounds from Vanillin and p-Aminoacetophenone Using Lime Juice as a Natural Acid

Catalyst and Their Utilization as Corrosion Inhibitors. *Advances in Social Sciences, Education and Humanities Research*, 529, 297-301.

Musa Husaini, Bishir Usman and Muhammad Bashir Ibrahim (2018) Evaluation of Corrosion Behaviour of Aluminum in Different Enviironment. *Bayero Journal of Pure and Applied Sciences* , 11(1), 88-92.

Musa Hussaini, Bishir Usman, Muhammad Bashir Ibrahim (2019) Study of corrosion inhibition of Aluminium in nitric acid solution using Anisaldehyde (4-methoxy benzaldehyde) as inhibitor. *Algerian Journal of Engineering and Technology* 01, 011 - 018.

Musa Hussaini, Umar Yunusa, Hussaina Aminu Ibrahim, Bishir Usman and Muhammad Bashir Ibrahim (2020) Corrosion inhibition of aluminium in phosphorric acid solution using glutaraldehyde as inhibitor. *Algerrian Journal of Chemical Engineering* 01, 12-21.

Nahle A., Salim R., El Hajjaji F., Aouad M. R., MessaliM., *et al.* (2021), Novel triazole derivatives as ecological corrosion inhibitors for mild steel in 1.0 M HCl: experimental & theoretical approach, *RSC Adv.*, 11, 4147–4162

Nura Ishaq and Magaji Ladan (2023) Triazole Derivatives as Corrosion Inhibitors on Iron (110) Surface: A Theoretical Study. *ChemSearch Journal* 14(1), 54 - 65.

Paul Ocheje Ameh, Ladan Magaji and Takuma Salihu (2012) Corrosion inhibition and adsorption behaviour for mild steel by Ficus glumosa gum H2SO4 solution. *African Journal of Pure and Applied Chemistry*, 6(7) , 100 - 106.

Pragnesh N Dave, Lakha V Chopda (2018) Schiff based corrosion inhibitors for metals in acidic environment : A review. *Material Science $ Engineering International Journal*, 2(6) , 258 - 267.

Siaka A.A, N. O. Eddy, S. O. Idris and L. Magaji (2014) Ampicillin potentials as Corrosion Inhibitor: fukui function calculations using B3-YLP exchange correlation. *Nigeria Journal of Chemical Research*, l (19), 12-25.

Usman Ishaq Shehu, Bishir Usman (2023) Corrosion Inhibition of Iron Using Silicate Base Molecules: A Computational Study. *Advanced Journal of Chemistry-Section A*, 6(4), 334-341.

Zarrouk A., Hammouti B., Al-Deyab S.S., R. Salghi, H. Zarrok, C. Jama, F. Bentiss (2012) Corrosion Inhibition Performance of 3,5-Diamino-1,2,4-triazole for Protection of Copper in Nitric Acid Solution, *Int. J. Electrochem. Sci.,* 7 N°7, 5997-6011.